



Multinuclear nuclear magnetic resonance and density functional theoretical studies on the structure of bisperoxovanadium complexes with bidentate donors

Birong Zeng^a, Riqiang Fu^b, Shuhui Cai^c, Jun Zhang^c, Zhong Chen^{c,*}

^a Department of Materials Science and Engineering, Fujian Key Laboratory of Plasma and Magnetic Resonance, Xiamen University, Xiamen 361005, China

^b Center for Interdisciplinary Magnetic Resonance, National High Magnetic Field Laboratory, 1800 East Paul Dirac Drive, Tallahassee, FL 32310, USA

^c Department of Physics, Fujian Key Laboratory of Plasma and Magnetic Resonance, State Key Laboratory of Physical Chemistry of Solid Surfaces, Xiamen University, Xiamen 361005, China

ARTICLE INFO

Article history:

Received 25 May 2010

Received in revised form 17 August 2010

Accepted 21 August 2010

Available online 26 August 2010

Keywords:

NMR spectroscopy

Bispermoxovanadium complex

Quantum chemistry

Coordination manner

ABSTRACT

Solid state and solution ^{51}V and ^{13}C NMR studies on four fundamental bisperoxovanadium complexes containing bidentate donor ligands were reported, together with DFT calculations of structural and NMR parameters. The ^{51}V solid-state NMR characterization of the four complexes with $[\text{VO}(\text{O}_2)_2\text{L}]^{n-}$ anion {abbr. bpVL, where L = oxalic acid dianion (ox), pyridine-2-carboxylic acid (pic), bipyridine (bipy), and 1,10-phenanthroline (phen)} show that the ligands have a significant effect on the electric-field gradient tensor, with the quadrupolar coupling constant ranging from 4.0 to 5.8 MHz. The experimental and theoretical results suggest that the vanadium center of bpVpic, bpVphen and bpVbipy in solid state and aqueous solution are all seven-coordinated except that bpVox is six-coordinated in aqueous solution. The steric space hindrance of the organic ligands and the bonding between vanadium with the coordination influences the activity of bpVL complexes.

© 2010 Elsevier B.V. All rights reserved.

1. Introduction

Bispermoxovanadium complexes are potent protein tyrosine phosphatase (PTPase) inhibitors with insulin-mimetic properties and could be developed into a new kind of oral drug for the treatment of diabetes [1–4]. Recently, this kind of compounds has received considerable attention [5–7]. The design and synthesis of more effective bisperoxovanadium compounds have become one of the most challenging fields in vanadium chemistry [8–11]. However, the knowledge of the structure–function relationship and solution properties of the bisperoxovanadium complexes is still limited to date [12,13]. It is known that the coordination chemistry of vanadium compounds plays an important role in *in vitro* insulin-mimetic activity and *in vivo* antidiabetic blood glucose lowering activity [14–16]. X-ray studies show that many monomeric peroxovanadium complexes are commonly pentagonal bipyramidal with the peroxo groups generally bound in the equatorial plane relative to the axial oxo ligand. The remaining equatorial and apical positions in the coordination shell are occupied by other ligands [17]. In contrast, the structure and the coordination number of bisperoxovanadium complexes in aqueous solution are still unclear and controversial due to the possible geometric changes [18–20].

In the past decades, ^{51}V solid-state nuclear magnetic resonance (SSNMR) spectroscopy has become an important analytical tool for studying vanadium compounds [21–23]. The NMR techniques allow for obtaining the structural parameters, chemical shift anisotropy (CSA) and electric-field gradient (EFG), which represents the local environment and its distortion of the vanadium nucleus being studied [24–26]. The combined use of SSNMR and computational methods can provide unique structural information unavailable from single-crystal X-ray diffraction or other spectroscopic methods [27,28]. For example, the ^{51}V SSNMR and density functional theory (DFT) calculations were employed to obtain the quadrupolar coupling and chemical shift tensors of the vanadium active site in a 67.5 kDa vanadium chloroperoxidase, revealing a protonated state of the vanadate cofactor in the resting form [29]. They were also used to study a series of five-coordinated VO_2 -dipicolinate complexes to interpret the relationships between the coordination geometry, the change in ligands, and the NMR observables [30]. However, studies on the structural and NMR parameters of solid-state bisperoxovanadium complexes and their solution structures are still limited.

Four fundamental bisperoxovanadium complexes with $[\text{VO}(\text{O}_2)_2\text{L}]^{n-}$ anion {abbr. bpVL, where ligand L = oxalic acid dianion (ox), pyridine-2-carboxylic acid (pic), bipyridine (bipy), and 1,10-phenanthroline (phen), $n = 1–3$ determined by ligands}, have been proved to display remarkable inhibitory effects on the bovine heart tyrosine phosphatase (BHPTase) in previous report

* Corresponding author.

E-mail address: chenz@xmu.edu.cn (Z. Chen).

[31]. Their IC₅₀ values were 0.22, 0.28, 0.36 and 0.90 $\mu\text{mol/L}$ for bpVox, bpVpic, bpVbipy and bpVphen, respectively. It showed that the inhibitory activity of the four bpVL complexes on the BHPTase had the following order: bpVox > bpVpic > bpVbipy > bpVphen [31]. The four organic ligands represent three types of the coordination atomic pair (OO, ON and NN). In this paper, multinuclear (⁵¹V and ¹³C) NMR was employed to characterize the four bpVL complexes in order to obtain more information about their structures in solid state and aqueous solution. DFT calculations were performed to elucidate the experimental observations.

2. Experimental

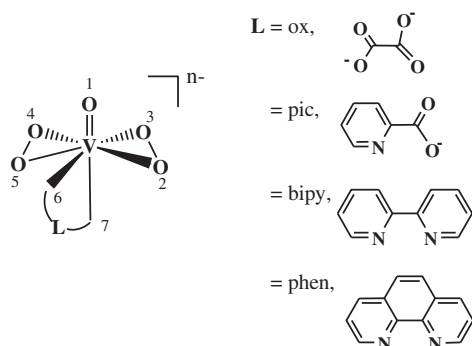
2.1. Experimental details

The four bpVL complexes bpVox, bpVpic, bpVphen and bpVbipy were prepared using the methods described previously [32–35]. The sketch structures of the four solid-state bpVL anion and ligands are shown in Scheme 1.

2.2. NMR measurements

The solid-state ⁵¹V NMR experiments were performed on a Bruker DRX 600 NMR spectrometer ($B_0 = 14.1$ T) where the ⁵¹V Larmor frequency is 157.7 MHz using a 2.5 mm Bruker double resonance MAS probe, and on a Bruker DMX 300 NMR spectrometer ($B_0 = 7.0$ T) where the ⁵¹V Larmor frequency is 78.8 MHz using a 4.0 mm Bruker double resonance MAS probe. The spinning speeds of ZrO₂ rotors were in the range of 10–30 kHz. The ⁵¹V isotropic chemical shifts were referenced to neat VOCl₃ (assigned to 0 ppm). The solid-state ¹³C MAS NMR spectra were recorded on the Bruker DMX 300 NMR spectrometer where the ¹³C Larmor frequency is 75.5 MHz. The samples were spun at 6.0 kHz using a 4.0 mm Bruker double resonance MAS probe. The ¹³C isotropic chemical shifts were referenced to the carbonyl carbon of glycine (assigned to 173.2 ppm). All lineshapes of the centerband and CSA sidebands were simulated through a MATLAB program.

The solution ⁵¹V and ¹³C NMR spectra were recorded on a Bruker AV 300 spectrometer ($B_0 = 7.0$ T). Routine parameters were used for the ¹³C NMR spectra, and DSS (trimethylsilylpropanesulfonic acid sodium salt) was used as an internal reference for the ¹³C chemical shifts. The ⁵¹V chemical shifts were measured relative to an external standard VOCl₃. A line broadening of 2 and 10 Hz was applied before Fourier transformation for all ¹³C and ⁵¹V spectra, respectively.



Scheme 1. Sketch structure and atomic numbering of solid-state bisperoxovanadium anions and ligands.

3. Computational details

The geometries of the four complexes were optimized using the B3LYP hybrid density functional, which includes a mixture of Hartree–Fock exchange with Beck88 exchange functional under generalized gradient approximation plus a mixture of Vosko–Wilk–Nusair local correlation functional and Lee–Yang–Parr non-local correlation functional [36,37]. Vibrational frequencies were calculated to ensure that a true local minimum (only real frequencies) was reached. For O, N, C, and H, 6-311+G(2d,p) basis set was used. For V atom, 6-31G* basis set with an additional f function was used. The ⁵¹V and ¹³C chemical shielding values were calculated based on the optimized geometries and crystal structures respectively. The solvent effects were further taken into account in aqueous solution by using polarizable continuum model PCM [38] on optimized geometries. The ⁵¹V and ¹³C chemical shifts were reported with respect to the reference compounds VOCl₃ and TMS optimized at the same level of theory respectively. All calculations were carried out with the GAUSSIAN 03 program suite [39].

4. Results and discussion

4.1. ⁵¹V NMR

For each of the four bpVL complexes, three different spinning rates were used to identify isotropic resonances. Fig. 1 shows the ⁵¹V MAS NMR spectra of the four bpVL complexes. The centerbands are positioned at –713, –748, –741, and –733 ppm, as indicated by the asterisks in the spectra, for bpVox, bpVpic, bpVbipy, and bpVphen, respectively. The lineshapes of the centerbands, which are independent of chemical shift anisotropies, strongly depend on the second-order quadrupolar interactions. The fitting of the centerband lineshapes (as shown in the inserts of Fig. 1) allows one to obtain the quadrupolar coupling constant C_Q , the EFG tensor asymmetry parameter η_Q , and the isotropic chemical shift δ_{iso} . The results are given in Table 1. For bpVpic, the centerband shows the typical line-shape of the second-order quadrupolar line broadening, as indicated in Fig. 1b. However, for other three compounds, such a typical line-shape is not visible in the centerbands at 14.1 T. In order to verify the simulation results, we repeated these measurements at 7.0 T, as shown in Fig. 2. At a lower field, the centerbands for bpVox, bpVpic, bpVbipy, and bpVphen, as indicated by the asterisks, are positioned at –717, –756, –744, and –736 ppm, respectively. Importantly, the typical line-shape due to the second-order quadrupolar interaction becomes visible at the lower field, although the sensitivity at 7.0 T is much worse than at 14.1 T. The fittings with the same parameters obtained from Fig. 1 show good agreement with the experimental spectra, as illustrated in the inserts of Fig. 2. Note that, the maximum spectral width on this instrument was 200 kHz, so that the spinning sidebands of the satellite transition outside the spectral window were folded into the spectra, as indicated by the negative sidebands.

Since the shape of the spinning sideband manifold in Fig. 1 is not dominated by CSA, it is not possible to extract the CSA values from those sidebands without the knowledge of the EFG tensor and its relative orientation with respect to the chemical shift tensor. In order to simplify the data analyses, we set the sample rotation axis slightly off the magic angle. As a result, the spinning sidebands of the satellite transition become too broad to be observed in the spectra, while the width of the central transition sidebands is almost not affected by the off-MAS. As shown in Fig. 3a, the off-MAS spinning sidebands are now dominated by the large CSA. Although the lineshapes of the off-MAS spinning sidebands strongly depend on the EFG tensor and its orientation with respect to the chemical shift tensor, the integral intensities of the off-MAS

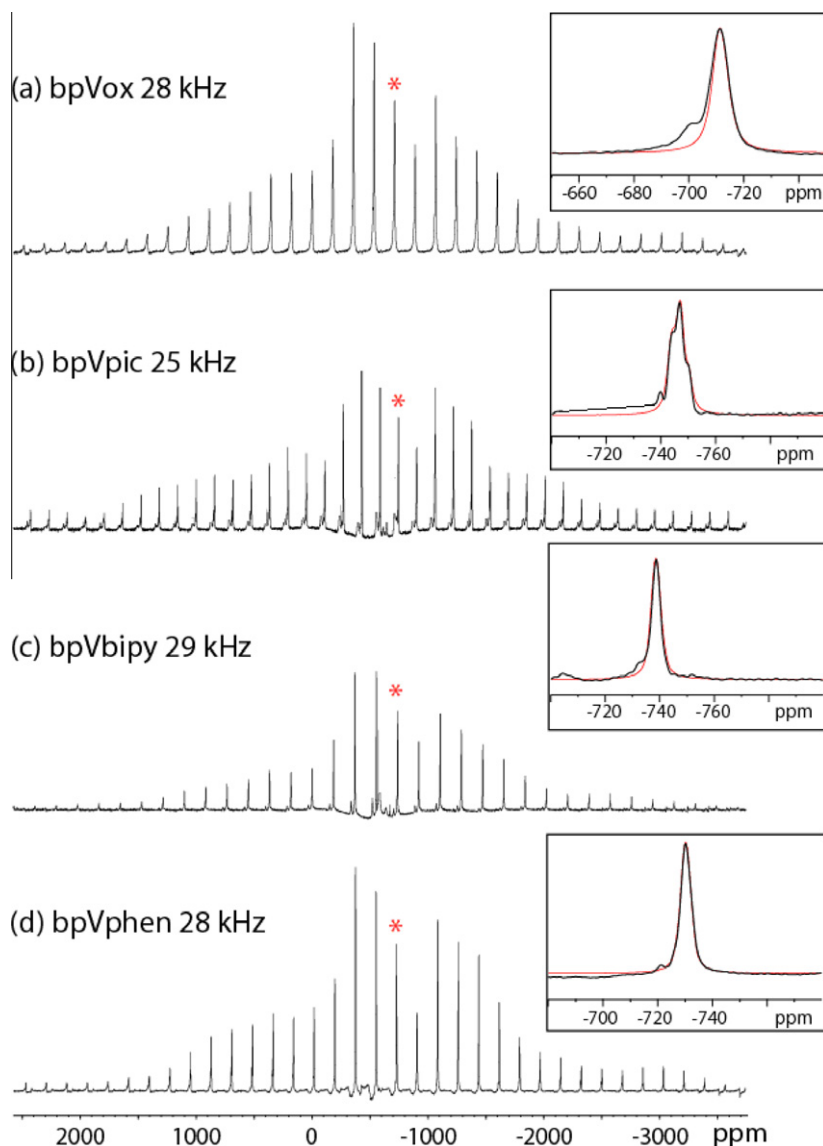


Fig. 1. Solid-state ^{51}V MAS NMR spectra of the four bisperoxovanadium complexes recorded at 14.1 T. The red traces are the fits. (For interpretation of the references to colour in this figure legend, the reader is referred to the web version of this article.)

Table 1
Solid-state ^{51}V NMR parameters of the four bisperoxovanadium complexes.

Compound	$C_Q \pm 0.5$	$C_{Q,\text{cal}} \pm 0.1$	$\eta_Q \pm 0.10$	$\eta_{Q,\text{cal}} \pm 0.05$	$\delta_{\text{iso}} \pm 5$	$\delta_{\text{iso,cal}}$	$\delta_{\text{aniso}} \pm 30$	δ_{11}	δ_{22}	δ_{33}	$\delta_{\sigma} \pm 30$	$\eta_{\text{CS}} \pm 0.05$	$\eta_{\text{CS,cal}} \pm 0.05$
bpVox	4.8	3.8	0.90	1.00	−704	−757	−920	−175	−313	−1624	−929	0.15	0.10
bpVpic	5.8	4.3	0.35	0.57	−735	−734	−950	−231	−351	−1620	−856	0.00	0.07
bpVbipy	4.0	4.2	1.00	1.00	−732	−692	−920	−167	−280	−1628	−937	0.00	0.07
bpVphen	4.0	5.5	1.00	0.91	−725	−716	−950	−155	−329	−1664	−948	0.10	0.10

Note: the data for bpVox were copied from Ref. [41]. Isotropic chemical shifts δ_{iso} , quadrupolar couplings C_Q and η_Q , and chemical shielding anisotropies δ_{σ} and η_{CS} were obtained from numerical simulations of ^{51}V MAS NMR spectra and DFT calculations. The unit of C_Q is in MHz, and unit of δ is in ppm.

spinning sidebands are solely dependent on the CSA. Fig. 3b shows the simulated MAS chemical shift spectrum of bpVox based on the relative sideband integral intensities from Fig. 3a, yielding the CSA δ_{aniso} of $−920 \pm 30$ ppm and the asymmetry parameter for CSA tensor η_{CS} of 0.15 ± 0.05 . Table 1 lists the CSA values of the four bpVL complexes.

It can be seen from Table 1 that the variation of the ligand has an effect on the ^{51}V EFG tensor, with the experimental C_Q ranging from 4.0 to 5.8 MHz for the four bpVL complexes. The variation

trend is as follows: bpVbipy = bpVphen < bpVox < bpVpic. At the same time, η_Q ranges from 0.35 to 1.0. The larger quadrupolar coupling constant for the asymmetric coordination atomic pair (ON pair rather than OO or NN pair) suggests a more asymmetric charge distribution for bpVpic. Interestingly, the change of the ligand primarily affects the EFG tensor, while the δ_{aniso} , ranging from $−920$ to $−950$ ppm, does not vary significantly across the four complexes. This slight variation of δ_{aniso} is within the fitting error of ± 30 ppm, indicating rather subtle differences in the chemical

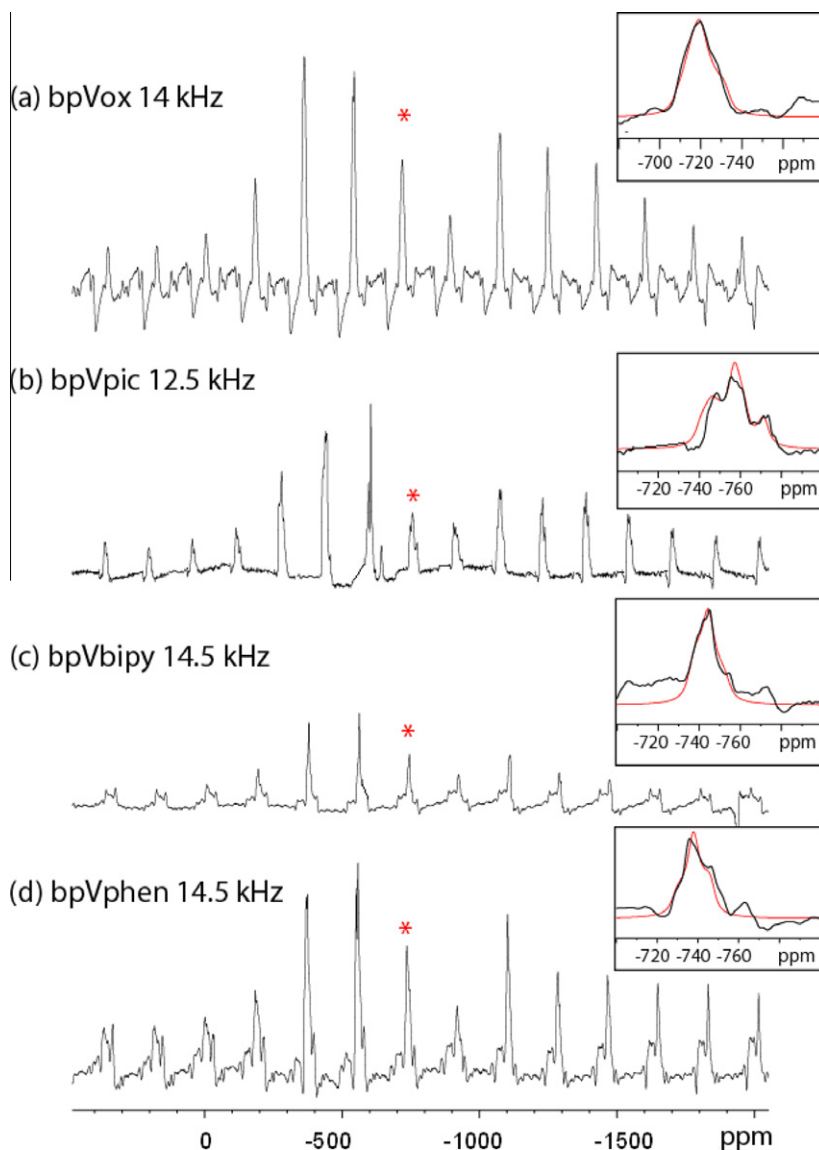


Fig. 2. Solid-state ^{51}V MAS NMR spectra of the four bisperoxovanadium complexes recorded at 7.0 T. The red traces are the fits. (For interpretation of the references to colour in this figure legend, the reader is referred to the web version of this article.)

environments of vanadium (V) centers, which is consistent with the structural similarities in the first coordination sphere of the vanadium centers, as shown in Scheme 1. The shape of the central transition sideband also indicates an axially symmetric CSA tensor, with η_{CS} close to zero. Such a low asymmetry of the CSA tensors is consistent with the predominant role of the $\text{V}=\text{O}$ bond in determining the magnetic shielding at the vanadium center [40].

The solution ^{51}V NMR spectra of the four complexes in D_2O with a concentration of 0.02 mol/L were recorded at room temperature for comparison. Their chemical shifts are -738 , -743 , -746 and -742 ppm, respectively. For all complexes, the ^{51}V isotropic chemical shifts between the solution and solid states differ by the range from 8 to 34 ppm. It may be attributed to a high sensitivity of the chemical shielding at the vanadium nucleus with respect to the change of its local environment. The magnitude of discrepancy is in the following order: δ_{bpVox} (34 ppm) $>$ δ_{bpVphen} (17 ppm) $>$ δ_{bpVbipy} (14 ppm) $>$ δ_{bpVpic} (8 ppm). Our previous work showed that the geometric structure of bpVox changes from seven-coordinated to six-coordinated when bpVox dissolves in water [41]. The largest discrepancy in ^{51}V isotropic chemical shifts between solid and

solution bpVox was due to the different geometries of the first coordination sphere of the vanadium center. For bpVphen, bpVbipy and bpVpic, the relatively small discrepancies may be attributed to the subtle differences introduced through secondary coordination effects [40]. This deduction is supported by the ^{13}C NMR spectra and further confirmed by DFT calculations (*vide infra*).

Variable temperature ^{51}V NMR experiments were performed to study the stability of bpVox and bpVphen in aqueous solution. The ^{51}V NMR spectra of bpVox and bpVphen with a concentration of 0.02 mol/L at temperatures ranging from 25 to 90 °C were recorded. For bpVphen, the ^{51}V resonance peak gradually moves towards low field as the temperature increases. A variation in the ^{51}V chemical shift can be attributed to a variation in the chemical environment around the vanadium nucleus. In solution the vanadium complexes interact with water molecules through the hydrogen bonding of the $-\text{V}=\text{O}/-\text{V}(\text{OO})$ to $\text{H}-\text{OH}$ [42]. Hydrogen bonding shifts the resonance signal of the proton to lower field (higher frequency), while it influences the chemical shielding of vanadium nucleus in $-\text{V}=\text{O}/-\text{V}(\text{OO})$, leading the resonance signal of the vanadium to a higher field. It is known that the strength of

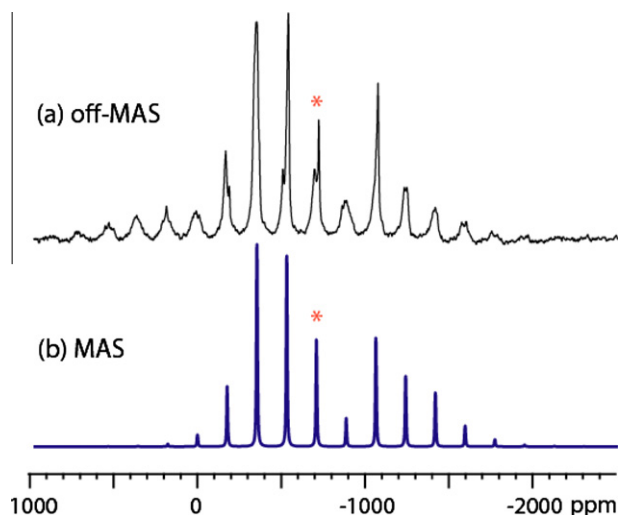


Fig. 3. (a) Solid-state ^{51}V off-MAS NMR spectrum of bpVox recorded at 14.1 T. (b) Simulated solid-state ^{51}V MAS NMR spectrum with $\delta_{\text{aniso}} = -920 \pm 30$ ppm and $\eta_{\text{CS}} = 0.15 \pm 0.05$.

hydrogen bond is sensitive to temperature. As temperature increases, the water molecular motion turns faster and the hydrogen bond is broken gradually. The reduction of hydrogen bond effect makes the peak of bpVphen move towards lower field. From 25 to 90 °C, the ^{51}V resonance peak of bpVphen shifts as large as 20 ppm (from -746 to -726 ppm), while its line-shape does not show any variation. When the temperature returns to 25 °C, the resonance peak returns to -746 ppm, implying that bpVphen is stable in this experimental temperature range. The thermal behavior of bpVox is the same as that of bpVphen when temperature is below 60 °C. The ^{51}V NMR peak of bpVox drifts from -738 to -724 ppm, and no additional peaks emerge in this period. When the temperature increases further, the peak at -724 ppm disappears gradually, and two new peaks steadily appear at -566 and -573 ppm, which were assigned to $\text{V}_4\text{O}_{12}^{4-}$ and $\text{V}_5\text{O}_{15}^{5-}$ respectively [43]. This indicates that bpVox is converted into $\text{V}_4\text{O}_{12}^{4-}$ and $\text{V}_5\text{O}_{15}^{5-}$. This conversion takes place completely at 90 °C. The ratio of the integral areas of $\text{V}_4\text{O}_{12}^{4-}$ to $\text{V}_5\text{O}_{15}^{5-}$ is 2.5:1. However, when cooling the sample back to room temperature, the sample does not form bpVox again and is still a mixture of polyvanadates. This implies that the conversion between bpVox and polyvanadates is irreversible. These experimental results show that bpVphen is thermally more stable than bpVox. Besides, bpVox is more readily to change than bpVphen at a same temperature. When bpVL complexes interact with BHPTase, the higher stability of bpVphen may make it more inactive than bpVox.

4.2. ^{13}C NMR

The solid-state ^{13}C MAS NMR spectra with a spinning rate of 6 kHz for the four bpVL complexes are shown in Fig. 4. For bpVox, the two carbon atoms of bpVox in solid-state evidently have different chemical environments. The peak at 167.8 ppm is assigned to the carbon linked with the oxygen at equatorial position (*cis* to oxo), and the peak at 165.6 ppm is assigned to the carbon linked with the oxygen at apical position (*trans* to oxo) [41]. Six peaks appear in the solid-state ^{13}C MAS NMR spectrum of bpVpic. The chemical shifts of the two carbon atoms adjacent to the nitrogen atom are 151.5 and 149.1 ppm. However, the two chemical shifts are both 148.5 ppm in free picolinic acid in solid-state NMR. Due to the symmetry, only five peaks could be observed in the ^{13}C NMR spectrum of bipyridine although the bipyridine molecule

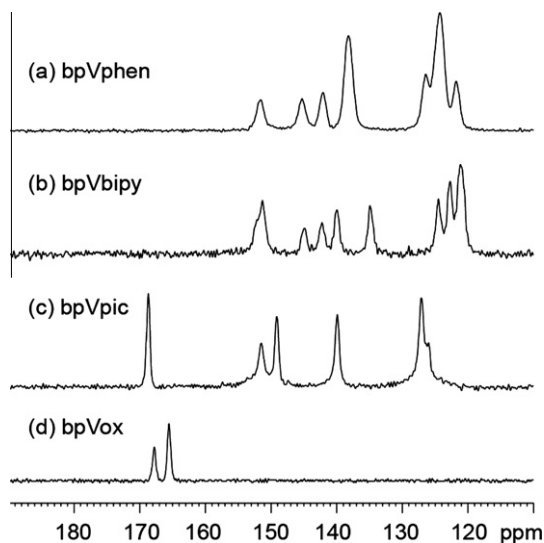


Fig. 4. Solid-state ^{13}C MAS NMR spectra of the four bisperoxovanadium complexes.

has 10 carbon atoms. Nine peaks were observed in the ^{13}C MAS NMR spectrum of bpVbipy, indicating that bipyridine is no longer symmetrical upon the complexation to $[\text{VO}(\text{O}_2)_2]^-$. As for bpVphen, it is too complicated to discuss because there are 12 carbon atoms in the molecule. These experimental results are consistent with the distorted pentagonal bipyramidal geometry of the four solid bpVL complexes. Besides, the chemical shifts of the two carbon atoms in bpVox are 168.0 and 173.4 ppm in aqueous solution. As $\text{Na}_2\text{C}_2\text{O}_4$ was added into the bpVox solution at room temperature, the intensity of the peak at 173.4 ppm was enhanced significantly. This indicates that the chemical environment of one of the carbons in bpVox is similar to that of the carbons in free $\text{C}_2\text{O}_4^{2-}$ in solution. The ^{13}C NMR shift of $\text{H}_2\text{C}_2\text{O}_4$ is 162.31 ppm. However, the ^{13}C NMR shift of $\text{Na}_2\text{C}_2\text{O}_4$ water solution is 173.9 ppm, which as expected is close to 173.4 ppm that reported for the not-coordinated carbonyl. Therefore, the peak at 173.4 ppm was assigned to the C-2 carbon that does not coordinate to V center. The chemical shift difference between the two carbon atoms of oxalate group is 2.2 ppm in solid state and 5.4 ppm in aqueous solution. This supported that the change of the coordination number of vanadium center in bpVox played an important role in the ^{13}C chemical shifts of bpVox in aqueous solution. Such obvious variation does not occur in the other three bpVL complexes. It implies again that the structural changes of bpVpic, bpVbipy and bpVphen after dissolution are less than that of bpVox.

4.3. DFT calculations

The DFT computations were performed to provide some theoretical evidences for a better understanding of experimental observations. Some optimized bond parameters of the four bpVL complexes are listed in Table 2, together with the experimental solid-state structure data. It can be seen that the optimized $\text{V}=\text{O}_1$ bond length is slightly shorter than the solid-state one for bpVox, bpVbipy and bpVphen, while it is opposite for bpVpic. For each complex, the four $\text{V}-\text{O}$ bond lengths ($\text{V}-\text{O}_2$, $\text{V}-\text{O}_3$, $\text{V}-\text{O}_4$ and $\text{V}-\text{O}_5$) are unequal in the solid state, and $\text{V}-\text{O}_3$ and $\text{V}-\text{O}_4$ are slightly shorter due to less steric influence from the ligand. In the optimized structures, the $\text{V}-\text{O}_2$ and $\text{V}-\text{O}_5$ bond lengths are almost equal, so are the $\text{V}-\text{O}_3$ and $\text{V}-\text{O}_4$ bond lengths. Similarly, the O_2-O_3 and O_4-O_5 bond lengths are unequal in solid state but equal in the optimized structure (data not shown). For the bonds between vanadium and coordination ligand, all of the optimized $\text{V}-\text{O}_6/\text{N}_6$

Table 2

Some geometric parameters of the solid state and optimized structures of the four bisperoxovanadium complexes (distances in Å and angles in degree).

Compound	Method	V=O ₁	V–O ₂	V–O ₃	V–O ₄	V–O ₅	V–O ₆ /N ₆	V–O ₇ /N ₇	O ₁ –V–O ₆ /N ₆	O ₁ –V–O ₇ /N ₇	O ₆ /N ₆ –V–O ₇ /N ₇
bpVox	experiment	1.622	1.934	1.866	1.856	1.911	2.060	2.251	90.3	164.4	74.1
	DFT	1.606	1.875	1.907	1.904	1.868	2.084	4.988	100.1	124.2	24.2
bpVpic	experiment	1.600	1.917	1.895	1.880	1.899	2.124(N)	2.290(O)	93.6	166.7	73.1
	DFT	1.616	1.868	1.873	1.873	1.868	2.305(N)	3.028(O)	90.6	152.5	62.0
bpVbipy	experiment	1.619	1.911	1.883	1.880	1.909	2.149	2.288	92.4	165.2	72.8
	DFT	1.607	1.901	1.871	1.871	1.901	2.233	2.435	92.1	160.6	68.5
bpVphen	experiment	1.613	1.906	1.878	1.875	1.880	2.143	2.347	94.1	166.1	72.1
	DFT	1.606	1.895	1.872	1.872	1.895	2.235	2.500	91.8	160.8	69.0

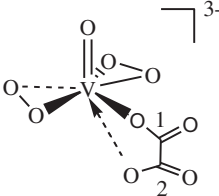
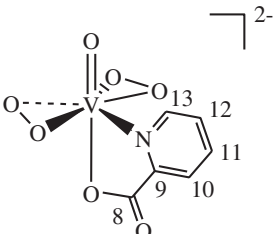
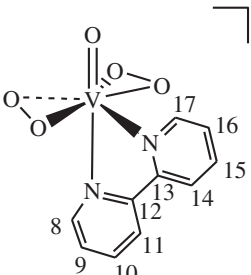
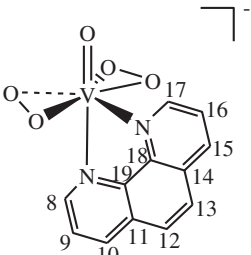
Note: the data for bpVox were copied from Ref. [41]. See Scheme 1 for atomic numbering.

and V–O₇/N₇ distances are longer than the corresponding ones in the solid state. Furthermore, the increases of the V–O₇/N₇ distances are generally much greater than the V–O₆/N₆ distances, especially for bpVox and bpVpic. The V–O₇ distance increases from 2.251 Å (solid state) to 4.988 Å for bpVox, and from 2.290 Å (solid state) to 3.028 Å for bpVpic. The bond angles related to the O₇/N₇ also change a lot in accordance. All these indicate that the [VO(O₂)₂][–] group and the V–O₆/N₆ and V–N₇ bonds are rather stable from

solid state to gas phase, while the V–O₇ bond is greatly weakened or even broken in gas phase, and possibly in aqueous solution too, due to the relatively flexible structure of the coordination groups in oxalate and piconlate and the weaker coordination capability of oxygen relatively to nitrogen.

The calculated ¹³C chemical shifts of the four bpVL complexes and their assignments [32] were listed in Table 3. The chemical shifts of C-1 and C-2 in solid-state bpVox were calculated to be

Table 3Comparison of the experimental and calculated ¹³C NMR chemical shifts of the four bisperoxovanadium complexes (in ppm).

Compound	Solid state		Aqueous solution		
	δ _{exp}	δ _{cal}	δ _{exp}	δ _{cal}	δ _{cal,pcm}
	167.8 (C-1)	168.6	168.0 (C-1)	184.8	183.7
	165.6 (C-2)	165.1	173.4 (C-2)	185.1	183.8
	168.7 (C-8)	168.7	171.9 (C-8)	174.8	172.9
	149.1 (C-9)	152.5	154.0 (C-9)	167.6	168.6
	127.1 (C-10)	118.2	130.8 (C-10)	130.3	135.4
	139.9 (C-11)	124.8	144.5 (C-11)	134.4	146.0
	126.0 (C-12)	113.6	128.2 (C-12)	119.2	131.6
	151.5 (C-13)	153.5	155.1 (C-13)	162.0	162.3
	142.2 (C-8)	150.4	148.9 (C-8)	163.0	161.4
	122.7 (C-9)	108.9	128.5 (C-9)	122.8	130.0
	134.9 (C-10)	120.4	142.0 (C-10)	133.5	143.2
	121.2 (C-11, C-14)	113.2	123.2 (C-11)	118.9	125.7
	145.0 (C-12)	162.4	151.6 (C-12)	156.4	155.5
	152.0 (C-13, C-17)	164.3	156.3 (C-13)	163.6	161.9
		114.1	125.5 (C-14)	121.2	128.2
	140.0 (C-15)	134.3	144.5 (C-15)	137.0	146.6
	124.5 (C-16)	117.7	129.3 (C-16)	122.5	130.2
		169.3	157.2 (C-17)	152.2	151.7
	151.5 (C-8)	157.2	156.8 (C-8)	149.2	150.1
	121.8 (C-9, C-16)	121.8	127.6 (C-9)	123.3	128.7
	138.2 (C-10, C-15, C-19)	128.6	143.1 (C-10)	131.6	140.9
	124.3 (C-11, C-12, C-13, C-14)	129.2	131.1 (C-11)	131.5	134.2
		128.5	128.6 (C-12)	130.6	134.0
		126.7	129.6 (C-13)	126.7	132.0
		130.7	132.1 (C-14)	131.9	135.2
		137.1	140.1 (C-15)	136.4	145.1
		123.4	128.0 (C-16)	122.2	128.3
		154.1	148.8 (C-17)	158.4	159.0
	145.3 (C-17)	152.9	146.5 (C-18)	154.1	151.4
	142.0 (C-18)	146.2	143.4 (C-19)	150.5	147.4

Note: the data for bpVox were copied from Ref. [41].

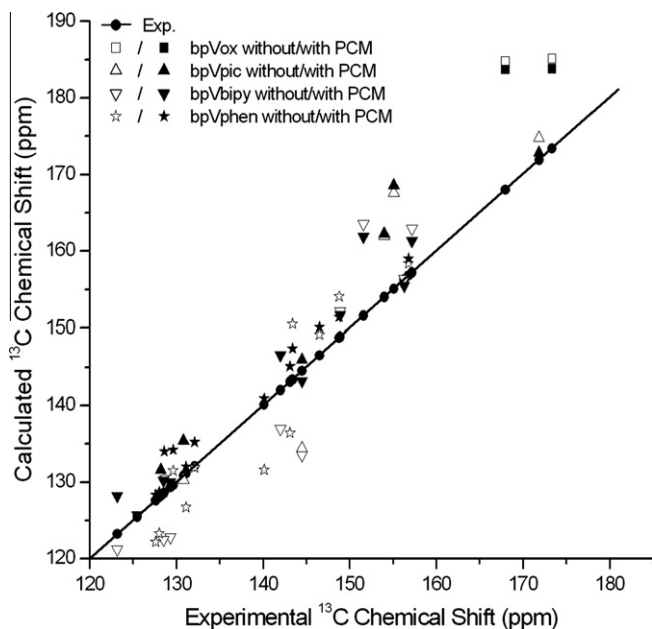


Fig. 5. Relationship of the calculated ^{13}C chemical shifts vs. experimental values for the four bisperoxovanadium complexes in aqueous solution. Solid black line with filled circle corresponds to perfect agreement. Different symbols represent different calculated results.

168.6 and 165.1 ppm respectively, in good agreement with the experimental measurement (167.8 and 165.6 ppm). Compared to the solid state, the deviations of the calculated values to the experimental ones become larger in aqueous solution. The relationship of the calculated ^{13}C chemical shifts to the experimental values for all four complexes in aqueous solution can be seen intuitively from Fig. 5. Obviously, the calculated chemical shifts may underestimate (more shielded) or overestimate (more deshielded) the experimental values before PCM correction. After PCM correction, most of the calculated values are overestimated the experimental values. The PCM data points are closer to the experimental ones, indicating a better agreement with the experimental measurements. Linear regression analysis of the theoretical ^{13}C chemical shifts for the four complexes gives the equation of $\delta_{\text{cal,pcm}} = 1.12 \times \delta_{\text{exp}} - 14.26$, and the correlation coefficient $R = 0.98$.

5. Conclusions

The four organic ligands (ox, pic, bipy and phen) coordinated in biologically active bpVL complexes have three types of the coordination atomic pair (OO, ON and NN). It has been found based on our solid-state NMR experiments and NMR simulation results that the different coordination agent results in a significant effect on the ^{51}V EFG tensor, with the experimental C_Q ranging from 4.0 to 5.8 MHz for the four bpVL complexes. The variation trend is as follows: $\text{bpVbipy} = \text{bpVphen} < \text{bpVox} < \text{bpVpic}$. Although the change of the ligand primarily affects the EFG tensor, it does not affect the CSA tensor significantly across the four complexes. The chemical shift anisotropies are about -920 ± 30 ppm and just show minor variation due to the ligand change. A small variation of δ_{aniso} is within the fitting error of ± 30 ppm, indicating rather subtle differences in the chemical environments of vanadium (V) centers, which is consistent with the structural similarities in the first coordination sphere of the vanadium center. The axially symmetric CSA tensor, with η_{CS} close to zero, is consistent with the predominant

role of the $\text{V}=\text{O}$ bond in determining the magnetic shielding at the vanadium center. As we know that, the inhibitory activity of the four bpVL complexes on the BHPTase has the following order: $\text{bpVox} > \text{bpVpic} > \text{bpVbipy} > \text{bpVphen}$, which cannot be explained merely by analyzing the solid-state structures of the four bpVL complexes. The information of the four bpVL complexes in aqueous solution should also be considered.

In solid state, the geometry for all of the four bpVL complexes is seven-coordinated, whereas bpVox is seven-coordinated in solid state and becomes six-coordinated in aqueous solution. Although the coordination manners of bpVpic, bpVphen and bpVbipy do not change from solid state to solution, the bond lengths between the vanadium and the coordinated atoms of the ligands are a bit longer in aqueous solution. A series of studies on the interactions between bisperoxovanadium complexes with some interaction organic molecules [2,6–8,10,31,32,44,45] have proved that, the coordinative unsaturated vanadium is related to its reactivity, and the most possible reaction mode of bpVox/bpVpic/bpVbipy with organic molecule includes the step in which organic molecule attacks the vanadium center of bpVox/bpVpic/bpVbipy from the opposite site to $-\text{V}=\text{O}$ and forms a transition species. The geometry of bpVox in aqueous solution and the small volume of ox ligand may be the possible reasons for the high activity of bpVox. For bpVpic, the elongation of the $\text{V}-\text{O}_7$ bond length in solution may benefit the vanadium center to be attacked easily by the organic molecule due to the big space. Besides, the coordination capability of ligands plays a role in the activity of bpVL complexes. According to the Petterson's report [46], the coordination capability of the aromatic N atom is better than that of the O atom. It can be seen that the coordination capability of pic ligand is stronger than that of ox ligand, but is weaker than that of bipy ligand. What's more, the volume of carboxylate group in bpVpic is smaller than that of pyridyl group in bpVbipy, which is helpful for organic molecule attacking the opposite site of $-\text{V}=\text{O}$ of bpVpic. The space effect and coordination capability as well as volume effect lead to the result that the inhibitory activity of bpVox and bpVpic on the BHPTase is stronger than that of bpVbipy. The space hindrance of phen ligand is greater than that of bipy ligand due to the rigid structure of phen. As for bpVphen, the interaction system of bpVphen and organic molecule cannot produce transition species because of the strong space hindrance of phen ligand, so the interaction depends on the molecular collision. Only high-energy molecules have the chances to interact with bpVphen and substitute the phen ligand. On the other hand, the π -electron system of phen ligand is greater than that of bipy ligand, which results in more π -antibonding orbitals and thus stronger coordination capability for phen ligand than for bipy ligand. All above factors make the inhibitory activity of bpVphen weaker than that of bpVbipy. In summary, the inhibitory activity of bpVphen is most inactive among the four bpVL complexes. However, the establishment of real structure–activity relationship of bisperoxovanadium complexes is very complicated and requires further investigation.

Acknowledgments

This work was partially supported by the Science Research Foundation of Ministry of Health & United Fujian Provincial Health and Education Project for Tackling the Key Research (WKJ2008–2–36) and the National Natural Science Foundation of China (10774125 and 20921120405). Some solid-state NMR measurements were performed at the National High Magnetic Field Laboratory (NHMFL) supported by the NSF Cooperative Agreement DMR-0654118 and the State of Florida.

References

- [1] A. Zorzano, M. Palacin, L. Marti, S. Garcia-Vicente, *J. Inorg. Biochem.* 103 (2009) 559.
- [2] B.R. Zeng, T.H. Shen, A.A. Wu, S.H. Cai, X.Y. Yu, X. Xu, Z. Chen, *J. Phys. Chem. A* 11 (2010) 5211.
- [3] J. Chen, C.G. Ostenson, *Pancreas* 30 (2005) 314.
- [4] K.H. Thompson, J. Lichter, C. Lebel, M.C. Scaife, J.H. McNeill, C. Orvig, *J. Inorg. Biochem.* 103 (2009) 554.
- [5] F.P. Ballistreri, C.G. Fortuna, A. Pappalardo, G.A. Tomaselli, R.M. Toscano, *J. Mol. Catal. A* 308 (2009) 56.
- [6] B.R. Zeng, X.B. Zhu, S.H. Cai, Z. Chen, *Spectrochim. Acta, Part A* 67 (2007) 202.
- [7] X.Y. Yu, R.H. Liu, H.L. Peng, H.W. Huang, X.F. Li, B.S. Zheng, P.G. Yi, Z. Chen, *Spectrochim. Acta, Part A* 75 (2010) 1095.
- [8] X.Y. Yu, S.H. Cai, Z. Chen, *J. Inorg. Biochem.* 99 (2005) 1945.
- [9] P. Hazarika, S. Sarmah, D. Kalita, N.S. Islam, *Transition Met. Chem.* 33 (2008) 69.
- [10] B.R. Zeng, X.B. Zhu, X.Y. Yu, S.H. Cai, Z. Chen, *Spectrochim. Acta, Part A* 69 (2008) 117.
- [11] J. Chrapova, P. Schwendt, D. Dudasova, J. Tatiersky, J. Marek, *Polyhedron* 27 (2008) 641.
- [12] S. Pacigova, R. Gyepes, J. Tatiersky, M. Sivak, *Dalton Trans.* (2008) 121.
- [13] L.L.G. Justino, M.L. Ramos, F. Nogueira, A. Sobral, C. Geraldes, M. Kaupp, H.D. Burrows, C. Fiolhais, V.M.S. Gil, *Inorg. Chem.* 47 (2008) 7317.
- [14] M.J. Pereira, E. Carvalho, J.W. Eriksson, D.C. Crans, M. Aureliano, *J. Inorg. Biochem.* 103 (2009) 1687.
- [15] E.J. Baran, *J. Inorg. Biochem.* 103 (2009) 547.
- [16] R. Garg, N. Fahmi, R.V. Singh, *Russ. J. Coord. Chem.* 33 (2007) 761.
- [17] V.S. Sergienko, *Crystallogr. Rep.* 49 (2004) 401.
- [18] I. Banyai, V. Conte, L. Pettersson, A. Silvagni, *Eur. J. Inorg. Chem.* (2008) 34.
- [19] D.C. Crans, H.J. Chen, O.P. Anderson, M.M. Miller, *J. Am. Chem. Soc.* 115 (1993) 6769.
- [20] I.V. Vrcsek, M. Birus, M. Buhl, *Inorg. Chem.* 46 (2007) 1488.
- [21] D. Zeng, H. Fang, A. Zheng, J. Xu, L. Chen, J. Yang, J. Wang, C. Ye, F. Deng, *J. Mol. Catal. A* 270 (2007) 257.
- [22] A. Fenn, M. Wächtler, T. Gutmann, H. Breitzke, A. Buchholz, I. Lippold, W. Plass, G. Buntkowsky, *Solid State Nucl. Magn. Reson.* 36 (2009) 192.
- [23] K.J. Ooms, S.E. Bolte, J.J. Smee, B. Baruah, D.C. Crans, T. Polenova, *Inorg. Chem.* 46 (2007) 9285.
- [24] K.J. Ooms, S.E. Bolte, B. Baruah, M.A. Choudhary, D.C. Crans, T. Polenova, *Dalton Trans.* (2009) 3262.
- [25] W. Huang, L. Todaro, G.P.A. Yap, R. Beer, L.C. Francesconi, T. Polenova, *J. Am. Chem. Soc.* 126 (2004) 11564.
- [26] N. Pooransingh, E. Pomerantseva, M. Ebel, S. Jantzen, D. Rehder, T. Polenova, *Inorg. Chem.* 42 (2003) 1256.
- [27] L.L.G. Justino, M.L. Ramos, M. Kaupp, H.D. Burrows, C. Fiolhais, V.M.S. Gil, *Dalton Trans.* (2009) 9735.
- [28] A. Schweitzer, T. Gutmann, M. Wachtler, H. Breitzke, A. Buchholz, W. Plass, G. Buntkowsky, *Solid State Nucl. Magn. Reson.* 34 (2008) 52.
- [29] N. Pooransingh-Margolis, R. Renirie, Z. Hasan, R. Wever, A.J. Vega, T. Polenova, *J. Am. Chem. Soc.* 128 (2006) 5190.
- [30] S.E. Bolte, K.J. Ooms, T. Polenova, B. Baruah, D.C. Crans, J.J. Smee, *J. Chem. Phys.* 128 (2008) 052317.
- [31] X.W. Zhou, Z. Chen, Q.X. Chen, J.L. Ye, P.Q. Huang, Q.Y. Wu, *Acta Biochim. Biophys. Sin.* 32 (2000) 133.
- [32] X.W. Zhou, J.L. Ye, Z. Chen, Z.W. Chen, L.J. Yu, P.Q. Huang, Q.Y. Wu, *Chin. J. Struct. Chem.* 19 (2000) 343.
- [33] D. Begin, F.W.B. Einstein, J. Field, *Inorg. Chem.* 14 (1975) 1785.
- [34] A. Shaver, J.B. Ng, D.A. Hall, B.S. Lum, B.I. Posner, *Inorg. Chem.* 32 (1993) 3109.
- [35] C. Djordjevic, N. Vuletic, M.L. Renslo, B.C. Puryear, R. Alimard, *Mol. Cell. Biochem.* 153 (1995) 25.
- [36] A.D. Becke, *J. Chem. Phys.* 98 (1993) 5648.
- [37] C. Lee, W. Yang, R.G. Parr, *Phys. Rev. B* 37 (1988) 785.
- [38] V. Barone, M. Cossi, J. Tomasi, *J. Chem. Phys.* 107 (1997) 3210.
- [39] M.J. Frisch, G.W. Trucks, H.B. Schlegel, G.E. Scuseria, M.A. Robb, J.R. Cheeseman, J.J.A. Montgomery, T. Vreven, K.N. Kudin, J.C. Burant, J.M. Millam, S.S. Iyengar, J. Tomasi, V. Barone, B. Mennucci, M. Cossi, G. Scalmani, N. Rega, G.A. Petersson, H. Nakatsuji, M. Hada, M. Ehara, K. Toyota, R. Fukuda, J. Hasegawa, M. Ishida, T. Nakajima, Y. Honda, O. Kitao, H. Nakai, M. Klene, X. Li, J.E. Knox, H.P. Hratchian, J.B. Cross, V. Bakken, C. Adamo, J. Jaramillo, R. Gomperts, R.E. Stratmann, O. Yazyev, A.J. Austin, R. Cammi, C. Pomelli, J.W. Ochterski, P.Y. Ayala, K. Morokuma, G.A. Voth, P. Salvador, J.J. Dannenberg, V.G. Zakrzewski, S. Dapprich, A.D. Daniels, M.C. Strain, O. Farkas, D.K. Malick, A.D. Rabuck, K. Raghavachari, J.B. Foresman, J.V. Ortiz, Q. Cui, A.G. Baboul, S. Clifford, J. Cioslowski, B.B. Stefanov, G. Liu, A. Liashenko, P. Piskorz, I. Komaromi, R.L. Martin, D.J. Fox, T. Keith, M.A. Al-Laham, C.Y. Peng, A. Nanayakkara, M. Challacombe, P.M.W. Gill, B. Johnson, W. Chen, M.W. Wong, C. Gonzalez, J.A. Pople, *GAUSSIAN 03*, Revision D.01, Gaussian Inc., Wallingford, CT, 2004.
- [40] S. Nica, A. Buchholz, M. Rudolph, A. Schweitzer, M. Wachtler, H. Breitzke, G. Buntkowsky, W. Plass, *Eur. J. Inorg. Chem.* (2008) 2350.
- [41] B.R. Zeng, J. Zhang, R. Fu, S.H. Cai, Z. Chen, *Inorg. Chem. Commun.* 12 (2009) 1259.
- [42] W. Plass, *Coord. Chem. Rev.* 237 (2003) 205.
- [43] D. Rehder, *Coord. Chem. Rev.* 252 (2008) 2209.
- [44] X.Y. Yu, D.H. Ji, R.H. Liu, F.X. Yang, J.A. Xie, J.M. Zhou, X.F. Li, P.G. Yi, *J. Coord. Chem.* 63 (2010) 1555.
- [45] X.Y. Yu, J. Zhang, S.H. Cai, P.G. Yi, Z. Chen, *Spectrochim. Acta, Part A* 72 (2009) 965.
- [46] L. Pettersson, I. Andersson, A. Gorzsas, *Coord. Chem. Rev.* 237 (2003) 77.